


Diesel Combustion Modeling and Simulation for Torque Estimation and Parameter Optimization

Master's thesis
performed in **Vehicular Systems**

by
Fredrik Jones, Christoffer Jezek

Reg nr: LiTH-ISY-EX -- 08/4072 -- SE

June 11, 2008

Presentationsdatum 2008-05-29 Publiceringsdatum 2008-06-11	Institution och avdelning Institutionen för systemteknik Department of Electrical Engineering	 Linköpings universitet
---	--	--

Språk _____ Svenska <input checked="" type="checkbox"/> Annat (ange nedan) Engelska _____ Antal sidor 54	Typ av publikation _____ Licentiatavhandling <input checked="" type="checkbox"/> Examensarbete _____ C-uppsats _____ D-uppsats _____ Rapport _____ Annat (ange nedan) _____	ISBN (licentiatavhandling) ISRN 08/4072 Serietitel (licentiatavhandling) Serienummer/ISSN (licentiatavhandling)
---	---	--

URL för elektronisk version http://urn.kb.se/resolve?urn=urn:nbn:se:liu:diva-12117

Publikationens titel Diesel Combustion Modeling and Simulation for Torque Estimation and Parameter Optimization. Författare Christoffer Jezek & Fredrik Jones
--

Abstract <p>The current interest regarding how to stop the global warming has put focus on the automobile industry and forced them to produce vehicles/engines that are more environmental friendly. This has led to the development of increasingly complex controlsystem of the engines. The introduction of <i>common-rail</i> systems in regular automotives increased the demand of physical models that in an accurate way can describe the complex cycle within the combustion chamber. With these models implemented it is possible to test new strategies on engine steering in a cost- and time efficient way.</p> <p>The main purpose with this report is to, build our own model based on the existing theoretical models in diesel engine combustion. The model has then been evaluated in a simulation environment using Matlab/Simulink. The model that has been implemented is a multi-zone type and is able to handle multiple injections.</p> <p>The model that this thesis results in can in a good way predict both pressure and torque generated in the cylinder. More investigation in how the parameter settings behave in other work-points must be done to enhance the models accuracy. There is also some work left to do in the validation of the model but to make this possible more experimental data must be accessible.</p>

Nyckelord Multi-Zone, Diesel Combustion Modeling, Simulation for Torque Estimation, Parameter Optimization
--

Diesel Combustion Modeling and Simulation for Torque Estimation and Parameter Optimization

Master's thesis

performed in **Vehicular Systems,**
Dept. of Electrical Engineering
at **Linköpings universitet**

by **Fredrik Jones, Christoffer Jezek**

Reg nr: LiTH-ISY-EX -- 08/4072 -- SE

Supervisor: **Per Öberg**

Linköpings Universitet

Richard Backman

GM Powertrain Sweden AB

Examiner: **Associate Professor Lars Eriksson**

Linköpings Universitet

Linköping, June 11, 2008

Abstract

The current interest regarding how to stop the global warming has put focus on the automobile industry and forced them to produce vehicles/engines that are more environmental friendly. This has led to the development of increasingly complex controlsystem of the engines. The introduction of *common-rail* systems in regular automotives increased the demand of physical models that in an accurate way can describe the complex cycle within the combustion chamber. With these models implemented it is possible to test new strategies on engine steering in a cost- and time efficient way.

The main purpose with this report is to, build our own model based on the existing theoretical models in diesel engine combustion. The model has then been evaluated in a simulation environment using Matlab/Simulink. The model that has been implemented is a multi-zone type and is able to handle multiple injections.

The model that this thesis results in can in a good way predict both pressure and torque generated in the cylinder. More investigation in how the parameter settings behave in other work-points must be done to enhance the models accuracy. There is also some work left to do in the validation of the model but to make this possible more experimental data must be accessible.

Sammanfattning

Dagens intresse av att hejda den globala uppvärmingen har satt fokus på att minska bränsleförbrukningen och utsläpp från alla fordon som drivs av fossila bränslen. Ett steg i denna utveckling har gjort att styrningen av motorer blir mer och mer avancerade. I och med introduktionen av *common-rail* system för dieselmotorer har efterfrågan ökat av fysikaliska modeller som på ett korrekt sätt kan beskriva det komplexa förloppet som sker i förbränningskammaren. Dessa modeller gör det möjligt att på ett kostnads- och tidseffektivt sätt testa nya strategier på motorstyrningen.

Huvudsyftet med denna rapport är att med hjälp av befintliga teoretiska modeller för dieselförbränning bygga upp en egen modell som baseras på dessa. Denna modell har sedan utvärderats i en simuleringsbar miljö och för detta ändamål har Matlab/Simulink använts. Modellen som har implementerats är av multizons-typ och klarar av att hantera multipla injektioner.

Den modell som denna rapport leder till kan på ett bra sätt skatta tryck och moment givet de mätdata som fanns tillgängliga. Det som behövs förbättras med modellen är att undersöka hur parametersättningen stämmer vid flera olika arbetspunkter. Det krävs även vidare arbete med verifiering av de olika parametrarna men för att detta skall kunna genomföras krävs mer experimentdata.

Keywords: Multi-Zone, Diesel Combustion Modeling, Simulation for Torque Estimation, Parameter Optimization

Preface

This Master's thesis has been performed at Linköpings Tekniska högskola in collaboration with General Motors Powertrain (GM) during fall 2007. At GM's request the thesis is based on a report made at the University of Salerno [2] presented at the SAE conference in 2005.

Objectives

The main objective with this thesis is to achieve a simulation model that simulates the pressure trace in the cylinder during a compression/combustion cycle. From the pressure trace the torque that is produced can be calculated. The computer model should be implemented in MATLAB/Simulink and must be able to handle multiple injections.

Limitations

In this thesis there exists areas that not have been considered:

- the swirl factor. For different geometry of the piston there will be different swirl factors.
- that wall wetting may occur during the injection.
- that the cylinder wall temperature changes. This is considered to be known.
- to evaluate the emissions that arise in the cylinder such as nitrogen oxides and soot formation.

Another limitation is that this model must be initialized with correct initial condition such as inlet pressure and desired injection profile.

Thesis outline

Chapter 1 A short introduction of diesel engine and the combustion process.

Chapter 2 Describes the theory behind diesel combustion in detail.

Chapter 3 Describes the chosen model approach and the implementation.

Chapter 4 Explains the theory behind the implemented models.

Chapter 5 Gives a general view of the implementation.

Chapter 6 Presents the validation of the models.

Chapter 7 Presents results and conclusions.

Acknowledgment

We have some persons we would like express our gratitude to:

Without the help from our supervisor PhD student Per Öberg this work would not been completed at all. The guidance he has given us and our countless discussion has been invaluable. We also want to thank examiner Lars Eriksson at Linköpings Universitet and Richard Backman at General Motors Powertrain. Last but not least we thank Caroline and Emma for proofreading the report.

Contents

Abstract	iii
Preface and Acknowledgment	iv
1 Introduction	1
2 Background	2
2.1 Diesel engine	2
2.2 Diesel combustion	3
2.3 Diesel oil	5
3 The selected model	6
3.1 Model Structure	6
3.1.1 Model approaches	6
3.1.2 Implemented multi-zone model	7
3.1.3 The zones	7
3.1.4 Simulation of the model	8
3.1.5 Initial conditions	11
4 Theory behind the models	12
4.1 Thermodynamic model	12
4.1.1 Implementation form of the equations	13
4.2 Fuel injection model	15
4.3 Fuel spray	16
4.3.1 Fuel spray submodel	17
4.4 Fuel evaporation submodel	19
4.5 Combustion submodel	19
4.6 Heat transfer submodel	20
5 Implementation	22
5.1 General view	22
5.2 Simulink	22
5.3 S-functions	23
5.4 Solver	23

5.5	psPack	23
5.5.1	Thermal Properties	24
6	Validation	25
6.1	Comments about the Validation	25
6.2	Fuel injection	25
6.3	Fuel spray validation	26
6.4	Fuel evaporation model	28
6.5	Evaporation and combustion submodel	30
6.6	Heat transfer model	32
6.7	Thermal properties	33
6.8	Heat release analysis	33
6.9	Pressure	36
6.10	In-cylinder temperature	37
7	Results and Conclusions	39
7.1	Results	39
7.2	Conclusions	40
7.3	Future work	41
8	References	43
	Notation	45
A	Derivation of air entrainment rate and thermodynamic model	46
A.1	Air entrainment rate	46
A.2	Thermodynamic Equations	47
A.2.1	Energy at equilibrium	47
A.2.2	Energy with a frozen mixture	48
A.2.3	State equation - the ideal gas law	49
B	Sensitivity plots	50

Chapter 1

Introduction

After the introduction of common rail systems¹, the interest of diesel engines for automotive application has dramatically grown. A strong increase in fuel economy and significant reduction of emissions as well as combustion noise has been achieved, thanks to both optimized fuel strategies and improved fuel injection technology. The largest improvements have occurred in injection time response, injection pressure and nozzle characteristics. This has made it possible to use multiple injections (up to five or more) and has enhanced the fuel atomization. These improvements have resulted in a cleaner and more efficient combustion with benefits on emissions and fuel consumption.

In order to increase the advantages due to the implementation of multiple injections on common rail diesel engines appropriate engine control strategies have to be developed. In this thesis a diesel engine combustion simulation model is developed that is based on the report *Thermodynamic Modeling of Jet formation and Combustion in Common Rail Multi-Jet Diesel Engines*, see [2]. This simulation model will make it possible to test and validate new injection strategies instead of making expensive and time consuming experiments.

The complexity of the combustion due to turbulent fuel-air mixing makes it difficult to make a model with high accuracy and low computational time; a trade-off has to be made between these two. Single zone models based on empirical heat release laws could be used to simulate SI² engine performance and emissions but are inadequate to simulate the heterogeneous characteristics of the CI³ diesel combustion. In order to increase the accuracy in the simulation, the approach in the implementation is to use a multi-zone model.

¹Direct diesel injection, featuring high pressure injection with individual solenoid valves

²Spark Ignited

³Compression Ignited

Chapter 2

Background

This chapter is an introduction to the background theory of diesel engine and diesel combustion process.

2.1 Diesel engine

In mechanical terms, the internal construction of a diesel engine is similar to its gasoline counterpart-components e.g. pistons, connecting rods and a crankshaft are present in both. The different parts in the engine are shown in figure 2.1. Equal to a gasoline engine, a diesel engine operates in a four-stroke cycle (similar to the gasoline unit's Otto cycle). The principal differences lie in the handling of air and fuel, and the method of ignition.[10]

A diesel engine relies upon compression ignition (CI) to burn its fuel, instead of the spark plug used in a gasoline engine. The compression phase can be seen in figure 2.1 B. If air is compressed to a high degree, its temperature will increase to a point where fuel will burn upon contact with the air.[11]

Unlike a gasoline engine, which draws a fuel-air mixture into the cylinder during the intake stroke, the diesel engine aspirates air alone. Figure 2.1 A shows how the air is inhaled into the cylinder during the intake phase. Following intake, the cylinder is sealed as the intake valve is closed. The air charge is highly compressed to heat the charge to the temperature required for ignition. Whereas a gasoline engine's compression ratio rarely is greater than 11:1 to avoid damaging preignition, a diesel engine's compression ratio is usually between 16:1 and 25:1. This extremely high level of compression causes the air temperature to increase up to 700-900 degrees Celsius.[10]

As the piston approaches top-dead-center (TDC), diesel-fuel oil is injected into the cylinder at high pressure, causing the fuel charge to be atomized. The

injection of diesel-fuel during the end of compression is illustrated in figure 2.1 B. As a result to the high air temperature in the cylinder, ignition instantly occurs, causing a rapid and considerable increase in cylinder temperature and pressure (generating the characteristic diesel "knock"). The piston is driven downward with great force, pushing on the connecting rod and turning the crankshaft, as seen in figure 2.1 C.[10]

When the piston approach bottom-dead-center (BDC) the spent combustion gases are expelled from the cylinder to prepare for the next cycle. In figure 2.1 D it is shown that the exhaust valve is opened and the exhaust gases are expelled. In many cases, the exhaust gases will be used to drive a turbocharger, which will increase the volume of the intake air charge. This results in a cleaner combustion and greater efficiency. Another use of the exhaust gas is to recycle it and mix it with the fresh air, called EGR¹. This is another step to decrease the emissions. [10], [11]

Another big difference between the diesel- and gasoline engine is that the diesel engine works with excess air and there exists no throttle. This results in a much lower pumping loss² and is a great advantage for the diesel engine.[1]

2.2 Diesel combustion

The essential features of the compression-ignition or diesel engine combustion process can be described as follows. Fuel is injected into the engine cylinder toward the end of compression stroke, just before the desired start of combustion. The fuel is injected at a very high velocity, due to the high pressure in the fuel injection system.[1]

The liquid fuel is usually injected as one or more jets through small orifices or nozzles in the injector tip, thereafter the fuel jet atomizes into small droplets and penetrates into the combustion chamber. The fuel vaporizes and mixes with the hot in-cylinder air. Since the air temperature and pressure are above the fuel's ignition point, spontaneous ignition of parts of the mixed fuel and air occurs after a delay on just a few crank angle degrees. This is a phenomena of stratified combustion. [1]

The cylinder pressure increases rapidly as combustion of the fuel-air mixture occurs. The consequent compression of the unburned parts shortens the delay before ignition of the fuel and air, which has been mixed within combustible limits, that then burns rapidly. The increasing temperature and pressure also reduces the evaporation time of the remaining liquid fuel. Injection continues until the desired amount of diesel-fuel has entered the cylinder.[4]

¹Exhaust Gas Recycling

²I.e energy loss.

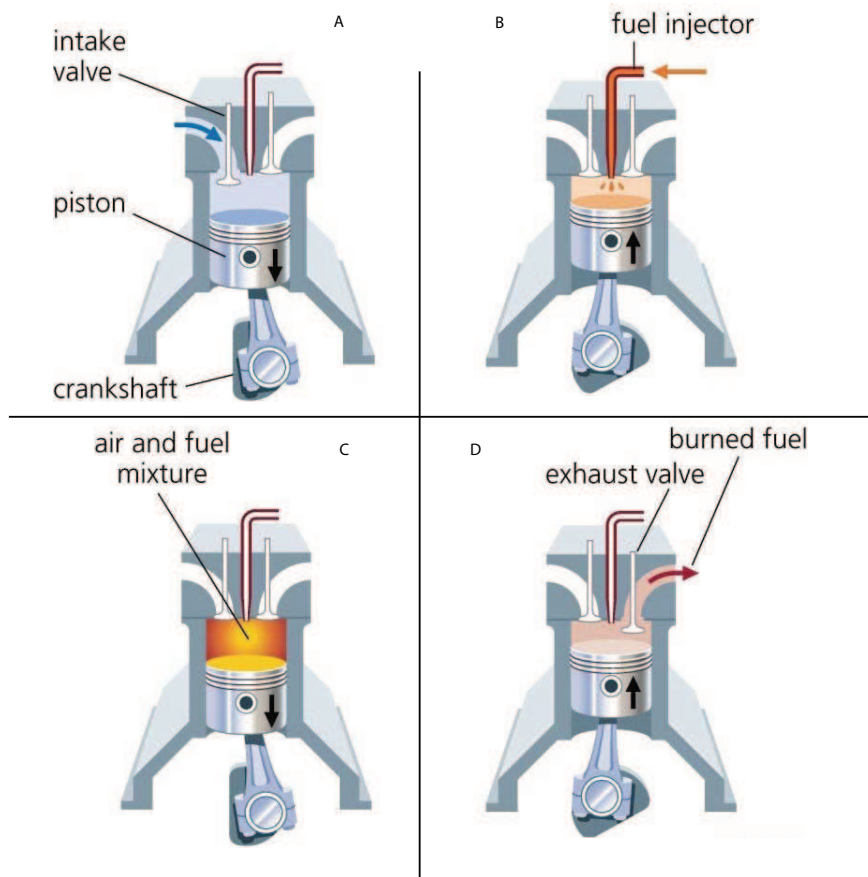


Figure 2.1: The different phases of a four stroke diesel engine.

The steep pressure rise, that originate from the ignition of the premixed fuel-air vapors is the source of the characteristic diesel engine combustion sound also known as knock. To prevent this steep pressure rise (knock) from occurring and to keep oxides of nitrogen (NO_x) emissions low a technique with small pre-injections before the main injection is often used. This results in a smother rise in cylinder pressure, which reduces the noise. Another result is that the global temperature is decreased which lowers the (NO_x) emissions.[1], [2]

Another possibility is to use injections after the main injection i.e. post-injection. The main idea with this post-injection is to reduce foremost the

soot but also (NO_x) due to a second burn of the incomplete combusted gas. In figure 2.2 a typical injection profile with both pre- and post-injections is presented. [4]

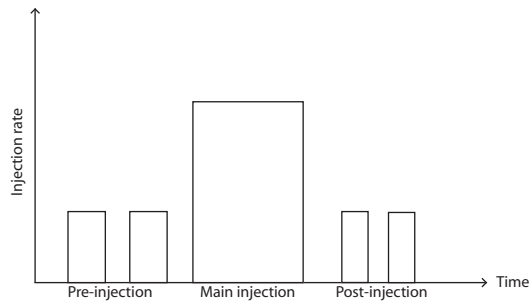


Figure 2.2: Principle of a typical multiple injections.

2.3 Diesel oil

In an engine point of view, the important characteristics in diesel oils appear to be ignition quality, density, heat of combustion, volatility, cleanliness and noncorrosiveness. As density and heat of combustion depend almost entirely on molecular weight it is impossible to secure appreciable departures from these two qualities as they are strongly correlated. With a given density the volatility, viscosity and ignition delay (cetane number) tend to change together. This is because they are all sensitive to molecular arrangement as well as to molecular size. All these relationships makes it very difficult to determine how one of these qualities alone effects the engine performance.[7]

The term *ignition quality*, loosely cover the ignition-temperature-versus-delay characteristics of a fuel when used in an engine. At a given speed, compression ratio, air inlet and jacket temperature, a good ignition quality means a short delay angle. Effects of the ignition quality in engine performance is the improvement in cold-starting characteristics and engine roughness. The engine roughness applies to the intensity of vibration of various engine parts caused by high rates of pressure rise in the cylinders.[7]

Chapter 3

The selected model

This chapter presents the model approach and which assumptions that have been made.

3.1 Model Structure

Due to the complexity of the diesel engine combustion and the turbulent fuel-air-mixing it is hard to develop a model that is accurate enough but that does not have too long computational time. There exists different approaches to implement a diesel combustion model i.e. single-zone, multi-zone and multi-dimensional. To get an model that is accurate enough, has a acceptable simulation time and has a complexity level that reflects the timeframe of this thesis, a multi-zone model has been selected. [4]

3.1.1 Model approaches

The different model approaches can be summarized as followed:

- **Single-zone.** A single-zone model is often used if there exists a need to have a fast and preliminary analysis of the engine performance. Single-zone models assume that the cylinder charge is uniform in both composition and temperature, at all time during the cycle. This approach is often used when simulation is made of a gasoline engine due to the homogeneous combustion. To use a single-zone model in the diesel case the model must be based on empirical heat-release laws. This approach need a wide identification analysis. Therefore is this approach excluded in this thesis. [4]
- **Multi-dimensional.** A multi-dimensional model, resolve the space of the cylinder on a fine grid, thus providing a great amount of special information. This approach has its downside in computational time

and need of storage space. Therefore this approach is also excluded in our thesis. [4]

- **Multi-zone.** As an intermediate step between single-zone and multi-dimensional models, multi-zone models can be effectively used to model diesel engine combustion systems. Selecting the multi-zone approach the advantages of single- and multidimensional models can be combined. By implementing a multi-zone model all the information needed is obtained in a reasonable time. The information given by the model is sufficient to achieve the thesis objectives. Therefore this approach is used in this thesis. [4]

3.1.2 Implemented multi-zone model

The multi-zone selected is based on the article *Thermodynamic modeling of jet formation and combustion in common rail multijet diesel engines* and is able to handle multiple injections. The article presents model for the fuel evaporation, air entrainment and combustion. The presented models for fuel evaporation and combustion is based on semi empirical expressions that only considers a mass rate.[2]

An analytical thermodynamical model is also presented but is not used in this thesis. In the package psPack¹ there exists a thermodynamical solver that handle multiple zones and therefore is this solver used instead. A fuel injection model has to be implemented from another source due to lack of that kind of model in [2]. These models will all be submodels in the entire model. There will be communication between the submodels and together these submodels will work as a unit. Figure 3.1 shows a hierarchy view of how the entire model is built and in figure 3.2 it is shown a flowchart over the different submodels that is implemented and how they interact with the thermodynamical model.

3.1.3 The zones

The multi-zone model is divided in the following zones: liquid-zone (l), air-zone (a), prepared-zone (p) and burned-zone (b). All diesel-fuel that's in a liquid state is placed in the *liquid-zone*. The liquid-zone is seen as an incompressible liquid and is therefore excluded from the thermodynamic model. The liquid zone will only occupy a known volume in the combustion chamber. When the injected diesel-fuel vaporizes due to heat and high pressure it transfers to the *prepared-zone*. All fresh air, i.e. air that is not yet burned, is placed in the *air-zone*. When the fresh air and the vaporized fuel react (burns) the burned gas transfers to the *burned-zone*.

¹see chapter 5

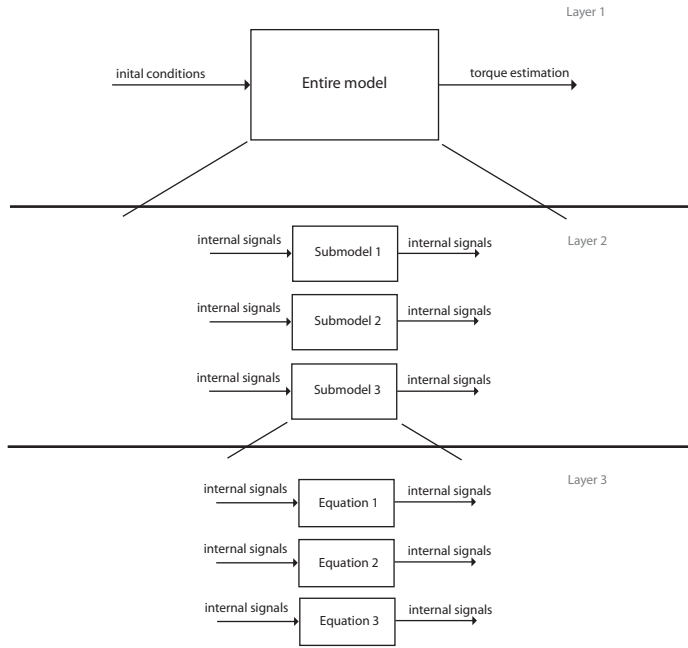


Figure 3.1: Hierarchy view of the models.

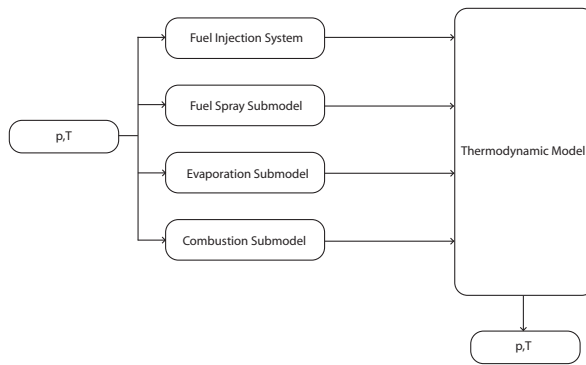


Figure 3.2: Flowchart over the implemented submodels.

3.1.4 Simulation of the model

To implement the model in a simulation environment the simulation process is divided into two steps.

- **Step 1** Step one (compression) occurs immediately after IVC² and no injection of fuel has yet been done. Therefore there only exists fresh air, EGR and in-cylinder residual gas. This gas composition is considered as a fully mixed homogenous gas with the same pressure and temperature in the whole cylinder. This is illustrated in figure 3.3. In this step the simulation uses the following states:

$$\text{States}(\text{step1}) = (p_{global} \quad V_{global} \quad T_{global}) \quad (3.1)$$

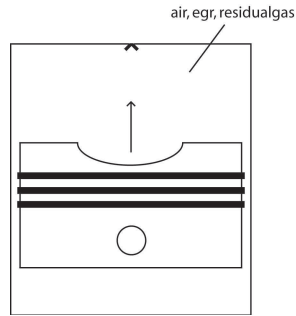


Figure 3.3: Compression with the homogeneous gas with air, egr and residual-gas.

- **Step 2** After the compression phase (step 1) comes the combustion phase (step 2). In step two the fuel injection system is activated. At this point the cylinder is divided in four different zones. For each one of the simulated zones are also the unique thermal properties calculated. This results in following continuous states when simulating step 2:

$$\text{States}(\text{step2}) = (p_{global} \quad V_a \quad T_a \quad V_p \quad T_p \quad V_b \quad T_b) \quad (3.2)$$

Where a stands for air, p for prepared and b for burned.

The *liquid-zone* consists of the injected fuel, the *air-zone* consists of fresh air, the *prepared-zone* consists of vaporized fuel and the *burned-zone* of combusted gas. Figure 3.4 gives the reader a roughly and illustrative picture of the heterogeneous development that takes action in the combustion chamber when an injection is made.

When the injection is active the injected fuel is considered as a liquid column and travels into the liquid-zone. The injected fuel then atomizes into small fine droplets and is entrained by the surrounding air. These droplets travel in a certain speed and are described by the fuel

²Intake Valve Closure

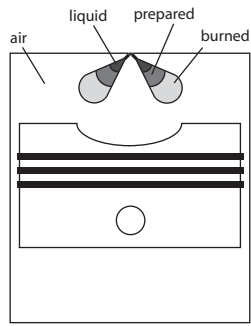


Figure 3.4: Illustrative picture of the jet formation.

spray submodel [2]. As the fuel evaporates and travels to the prepared-zone, air entrains and mix with evaporated fuel and then travels to the burned-zone. This means that mass flows between the zones. Figure 3.5 illustrate the **only** possible directions of the different mass flows over the zones.

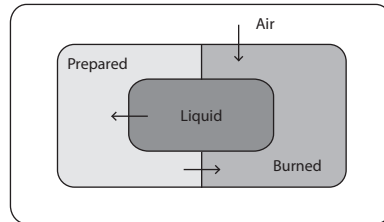


Figure 3.5: Mass flows between the different zones.

3.1.5 Initial conditions

There are a few initial conditions that must be defined before the simulation of the model can be started. The following table shows which variables and constants that must be initialized.

Constant name	Description
p_{im}	Intake pressure at IVC
T_{im}	Intake temperature at IVC
T_{fuel}	Temperature on the fuel
T_{wall}	Cylinder wall temperature
d_n	Nozzle diameter
$nr_{nozzles}$	Number of nozzles
N	Number of revolutions per minute
B	Cylinder bore
a	Crank radius
l	Connecting rod length
p_{rail}	Pressure in the common-rail
$pulse_{vector}$	Vector with the injection profile
x_{egr}	Defines the fraction of EGR

Chapter 4

Theory behind the models

This chapter presents the theory behind our implemented models.

4.1 Thermodynamic model

A thermodynamic model based on *A DAE Formulation and it's Numerical Solution for Multi-Zone thermodynamic models* [13] is presented in this chapter. The model is formulated as a differential algebraic equation model that is easy to transform numerically to a non-linear ordinary differential equation that can be solved. The resulting model gives the temperature and volume for each zone as well as the global pressure.

This multi-zone model is divided in the following zones:

1. Liquid
2. Air
3. Prepared
4. Burned

When the injection take place, the fuel jet forms a number of sprays, depending on the number of injection nozzle holes. This liquid-zone is considered as a liquid following these assumptions [2]:

- Incompressible liquid.
- No heat transfer from the zone.
- The liquid only occupies a known volume of the combustion chamber.

For the air-, prepared- and burned-zone the following assumptions are made:

- Uniform pressure into the combustion chamber at each time step.
- The change in system volume and mass transfer between the zones are known.
- Chemical equilibrium concentration in the burned zone.
- Frozen state in air- and prepared zone, i.e no reactions.
- Mixture of ideal gas in each zone, with thermodynamic properties depending on temperature, pressure and fuel-air ratio.
- Convective heat transfer for all zones.
- Radiative heat transfer for burned zone.
- No heat transfer between the zones.

In [13] a new approach in how to express and simplify the calculation of thermodynamic process is presented. In this report two new expressions, *well stirred reactor* and *well stirred mixer*, are introduced. The following equations are used to derive the expressions that describes a *well stirred reactor* and a *well stirred mixer*: There equation (4.1) describe the ideal gas law and equations (4.2) and (4.3) describes the energy in the gas mixture.

$$pV = nRT \quad (4.1)$$

$$U = n(p, T, \bar{x}_r) \sum_i \tilde{x}_i(p, T, \bar{x}_r) \tilde{u}_i(T) \quad \text{or.} \quad (4.2)$$

$$U = m \sum_i x_i(p, T, \bar{x}_r) u_i(T) \quad (4.3)$$

$$x_i = \frac{\tilde{x}_i M_i}{M} \quad (4.4)$$

there \bar{x}_r is the share of the respective atom among the reactants.

4.1.1 Implementation form of the equations

If the equations are studied for the *well stirred mixer* and the *well stirred reactor* -case it is shown that it is enough to implement the equation for *well stirred reactor*. The terms that differs between the two cases, for a gas that's not able to react, disappears when this equation form is used. It is therefore possible to conceal this information in the calculation of the different gas-properties. The full derivation from equations (4.1 – 4.4) to the equations implemented (4.5 – 4.7) can be further studied in appendix A2.

In equations (4.1 – 4.4) there is only one zone considered with the same gas properties from source to destination. This is not adequate when simulating combustion with a multi-zone model since the gas must be able to flow from one zone with a specific \bar{x} to another zone and then get a new \bar{x} .

When a mass is transferred from one zone to another zone it could either mix or react with the existing gas depending on what type of zone it travels to (e.g. *well stirred mixer* or *well stirred reactor*). A gas that transfers to a *well stirred mixer* is only mixed with the surrounding gas (e.g. no reactions at all). If the same gas instead is transferred to a *well stirred reactor* it reacts with the surrounding gas. The mass transfer between the zones defines a system of type open. In figure 4.1 an open system with mass transfer is shown.

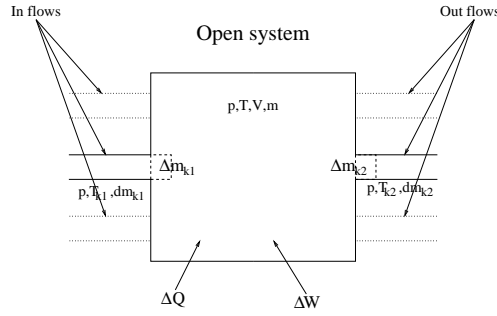


Figure 4.1: Definition of directions for an open system. Meantime the period Δt flows the masselement Δm_j in over the systemboundary concurrently as the energy ΔQ leads in and the work ΔW performs on the controlvolume.

One important detail by using this approach is that there will be a straightforward way to introduce the release of energy by using mass transfer between the zones in the equations. The entalphy, $h(p, \hat{T}_j, \hat{x}_{r,j})$, that one mass element brings to the new zone is not the same entalphy as if the mass element would have originated from the same type of zone with the exact amount of energy that is released at the combustion. If the $\hat{x}_{r,j}$ that includes entalphy in the expression is the same as $\bar{x}_{r,j}$, as in the source, then a mass transfer from *well stirred mixer* to *well stirred reactor* represents a combustion.

The equations that are needed and implemented are listed below.

$$p dV + \left(V - m T \frac{\partial R}{\partial p} \right) dp - m \left(R + T \frac{\partial R}{\partial T} \right) dT = \left(R + \nabla_{\bar{x}_r} R \cdot (\hat{x}_{r,d,j} - \bar{x}_r) \right) T dm_j \quad (4.5)$$

$$m c_v dT + m \frac{\partial u}{\partial p} dp + p dV = dQ + \left(\nabla_{\bar{\mathbf{x}}_r} u \cdot (\bar{\mathbf{x}}_r - \hat{\hat{x}}_{r,s,j}) + h(p, \hat{T}_{s,j}, \hat{\hat{x}}_{r,d,j}) - u \right) dm_j \quad (4.6)$$

$$d\bar{\mathbf{x}}_r = \frac{\bar{\mathbf{x}}_{r,d,j} - \bar{\mathbf{x}}_r}{m} dm_j \quad (4.7)$$

Here are

$$\hat{\chi}_{d,j} = \begin{cases} \chi_j & \text{For flow from outside to inside } (dm_j > 0) \\ \chi & \text{For flow from inside to outside } (dm_j \leq 0) \end{cases} \quad (4.8)$$

$$\hat{\chi}_{s,j} = \begin{cases} f(\chi_j) & \text{For flow from outside to inside } (dm_j > 0) \\ \chi & \text{For flow from inside to outside } (dm_j \leq 0) \end{cases} \quad (4.9)$$

$$u = u(p, T, \bar{\mathbf{x}}_r) = \sum_k x_k(p, T, \bar{\mathbf{x}}_r) u_k(T) \quad (4.10)$$

For $\chi \in \{T, \bar{\mathbf{x}}_r, x_k\}$.

$$\begin{pmatrix} 0 & 1 & 0 \\ a_1 & p & b_1 \\ c_1 & p & d_1 \end{pmatrix} \begin{pmatrix} dp \\ dV_1 \\ dT_1 \end{pmatrix} = \begin{pmatrix} dV \\ \left(R + \nabla_{\bar{\mathbf{x}}_r} R \cdot (\hat{\hat{x}}_{r,d,j} - \bar{\mathbf{x}}_r) \right) T dm_j \\ dQ + \left(\nabla_{\bar{\mathbf{x}}_r} u \cdot (\bar{\mathbf{x}}_r - \hat{\hat{x}}_{r,d,j}) + h(p, \hat{T}_{d,j}, \hat{\hat{x}}_{r,s,j}) - u \right) dm_j \end{pmatrix} \quad (4.11)$$

there

$$\begin{aligned} a_i &= V - m T \frac{\partial R}{\partial p} \\ b_i &= -m \left(R + T \frac{\partial R}{\partial T} \right) \\ c_i &= m \frac{\partial u}{\partial p} \\ d_i &= m c_v \end{aligned}$$

4.2 Fuel injection model

The figure 4.2 shows which signals that are sent into the submodel and what signals that comes out from the submodel.



Figure 4.2: In- and outsignals from the model

The model of fuel injection presented by Heywood [1] have been choosed and

implemented in the total model. The timing and rate of fuel injection affect the spray dynamics and combustion characteristics. If the pressure upstream of the injector nozzle can be measured or estimated and assuming the flow through each nozzle is quasi-steady, incompressible, and one dimensional, the mass flow rate of fuel through the nozzle, $\dot{m}_{f,inj}$, is given by:

$$\dot{m}_{f,inj} = C_D A_N \sqrt{2\rho_l \Delta p} \quad (4.12)$$

where A_N is the nozzle minimum area, C_D the discharge coefficient, ρ the density of liquid fuel, and ΔP the pressure drop across the nozzle. [1]

Since $\dot{m}_{f,inj} = A_N \rho_l u_i$, the fuel injection velocity at the nozzle tip u_i , can be expressed as:

$$u_i = C_D \sqrt{\frac{2\Delta p}{\rho_l}} \quad (4.13)$$

The discharge coefficient, C_D , have been investigated by [2] for several engine operating condition. As a result of their correlation analyses, the best compromise between accuracy and generalization for C_D is to use a function depending on the volume injected fuel q_{fuel} and engine speed N .

$$\begin{aligned} C_D &= a_1 - a_2 \cdot (q_{fuel} \cdot N) \quad \text{if } (q_{fuel} \cdot N) \geq \frac{1 - a_1}{a_2} \\ C_D &= 1 \quad \text{if } (q_{fuel} \cdot N) \leq \frac{1 - a_1}{a_2} \end{aligned} \quad (4.14)$$

Here $a_1 = 1.1774$, $a_2 = 3.95 \cdot 10^{-6}$, N is the engine speed in *rpm* and q_{fuel} is the volume injected in mm^3 . [2]

4.3 Fuel spray

At the start of injection, fuel begins to penetrate into the combustion chamber and high temperature air is entrained into the spray. The hot air evaporates the fuel and beyond a fixed length, known as the break-up length, no liquid fuel exists. The liquid length shortens slightly after the start of combustion but remains relatively constant until the end of injection. Beyond the break-up length, the rich premixed fuel and air continue to be heated until they react in the rich premixed reaction zone.[8]

Figure 4.3 shows an general overview of the fuel spray and its flame propagation. The products of rich combustion continue downstream and diffuse and mix radially outward until reaching the surrounding cylinder gases. At a location where the rich products and cylinder gases mix to produce a stoichiometric mixture, a diffusion flame is produced. The diffusion flame surrounds the jet in a thin turbulent sheet, which extends upstream toward the nozzle.

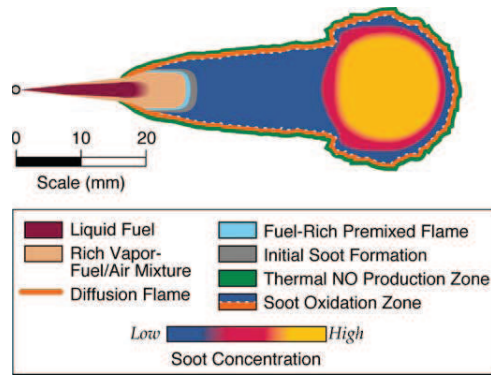


Figure 4.3: General view of a quasi-steady diesel combustion plume [8].

Soot is burned out and NO_x is produced on the outside of the diffusion flame, where temperatures are high and oxygen and nitrogen are abundant.[8]

Figure 4.4 shows the liquid phase and vapour phase of dme¹ in different

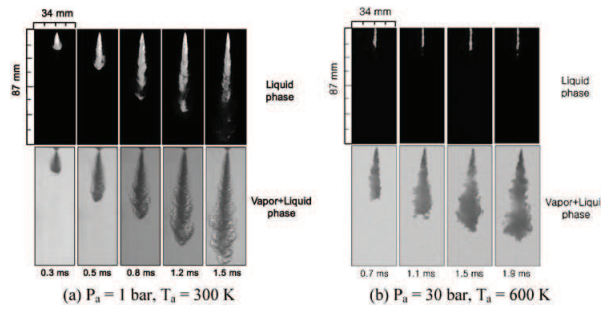


Figure 4.4: How liquid and vapour phase propagates in time.

conditions and how they propagates in time. The rail pressure was set to 400 bar and the injection duration was 3 ms. This figure shows in a distinct way the fuel spray behaviour with both liquid and vapour phase. [12]

4.3.1 Fuel spray submodel

Figure 4.5 shows which signals that are sent into the submodel and what signals that comes out from the submodel.

¹Dimethyl ether

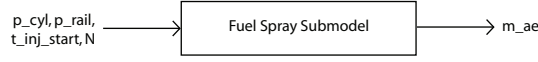


Figure 4.5: In- and outsignals from the fuel spray submodel

The fuel spray submodel describes the fuel motion from the nozzle hole into the combustion chamber. In every time step the model predicts the spray tip penetration s_{spray} and the spray velocity U_{spray} . It also predicts the mass of the entrained air $m_{a,e}$ into the fuel spray.

The injected fuel is assumed to be a liquid column that is connected to the liquid-zone. The liquid column travels through the nozzle hole exit at a constant velocity U_0 into the cylinder before the fuel spray breakup time, t_b , occurs. This relation is given by the following equations:

$$U_0 = C_D \sqrt{\frac{2\Delta p}{\rho_l}} \quad (4.15)$$

$$t_b = 4.351 \frac{\rho_l \cdot d_n}{C_D^2 \sqrt{\rho_a \Delta p}} \quad (4.16)$$

Where C_D is the discharge coefficient of the fuel injector, Δp is the pressure drop through the nozzle hole given in $[Pa]$, d_n is the nozzle hole diameter in $[mm]$, ρ_l is the density of the fuel and ρ_a is the air density in the air-zone.

After the break-up time, $t \geq t_b$, the fuel is assumed to be atomized into fine droplets. Then there will be a descending velocity of the fuel spray, U_{spray} :

$$U_{spray} = \frac{2.95}{2} \left(\frac{\Delta p}{\rho_a} \right)^{\frac{1}{4}} \sqrt{\frac{d_n}{t}} \quad (4.17)$$

To get the fuel spray break-up length, s_b , and the spray tip penetration s_{spray} are the two equations (4.15) and (4.17) integrated. The break-up length is defined as the length where the fuel spray liquid column atomizes into fine droplets and the spray tip penetration is the total length of the fuel spray that reaches into the combustion chamber. The equations for fuel break-up length and spray tip penetration is given by:

$$s_b(0 < t < t_b) = U_0 \cdot t = C_D \sqrt{\frac{2\Delta p}{\rho_l}} \cdot t \quad (4.18)$$

$$s_{spray}(t \geq t_b) = \frac{2.95}{2} \left(\frac{\Delta p}{\rho_a} \right)^{\frac{1}{4}} \sqrt{d_n} \cdot t \quad (4.19)$$

The mass of the entrained air, $m_{a,e}$ is described by the rate of air that entrains the atomized fuel which leads to the fuel droplets to evaporate. By using

the conservation of the momentum the prediction of the entrained air can be described by the following equation:

$$\dot{m}_{a,e} = - \frac{\int_0^t \dot{m}_{f,inj}(t) dt \cdot U_0}{(U_{spray}(t))^2} \cdot \dot{U}_{spray}(t) \quad (4.20)$$

Where $m_{f,inj}$ is the mass of the injected fuel. The integral describes the cumulative fuel mass injected and \dot{U}_{spray} is the gradient of the fuel spray velocity. For a more detailed description see appendix A1. [4], [2]

4.4 Fuel evaporation submodel

Figure 4.6 shows which signals that are sent into the submodel and what signals that comes out from the submodel. The evaporation submodel de-



Figure 4.6: In- and outsignals from the fuel evaporation submodel

scribes the evaporation process with a semi-empirical model proposed by Whitehouse and Way [3]. With this model approach some precision is lost due to the fact that the fuel atomization and vaporization are neglected. Fuel prepared-rate is only considered in this model.

The fuel is prepared after it has atomized and evaporated and then micro-mixed with the entrained air. The prepared mass flow is depending on the injected fuel at that time, on the entrained air (partial oxygen pressure in the prepared-zone) as well on the amount of fuel that is injected but not yet prepared. Following equation gives the relation between these dependencies:

$$\dot{m}_{f,p}(t) = C_1 \cdot \frac{180\omega}{\pi} \cdot \left(\int_0^t \dot{m}_{f,inj}(t) dt \right)^{\frac{1}{3}} (p_{O_2}(t))^{0.4} \cdot \left(\int_0^t \dot{m}_{f,inj}(t) dt - \int_0^t \dot{m}_{f,p}(t) dt \right)^{\frac{2}{3}} \quad (4.21)$$

where ω is engine speed in $\left[\frac{rad}{s}\right]$, p_{O_2} is the partial oxygen pressure in the air-zone in $[bar]$ and C_1 is a constant assumed equal to $0.035 \left[\frac{bar^{-0.4}}{deg}\right]$. [2], [3]

4.5 Combustion submodel

Figure 4.7 shows which signals that are sent into the submodel and what signals that comes out from the submodel. The combustion submodel also uses

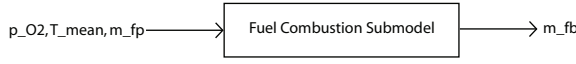


Figure 4.7: In- and outsignals from the combustion submodel

an semi-empirical model that is strongly connected to the fuel evaporation submodel. The mass of the burned fuel, $m_{f,b}$ is predicted by this model. There are two equations describing the rate of combustion. First is the rate of combustion, $\dot{m}_{f,b}$, and the second is the mean gas temperature of the three zones.

$$\dot{m}_{f,b}(t) = \frac{C_2 \cdot p_{O_2}}{N' \cdot \sqrt{T_{mean}(t)}} \cdot \frac{180\omega}{\pi} \cdot e^{\left(-\frac{T_A}{T(t)}\right)} \int_0^t (\dot{m}_{f,p}(t) - \dot{m}_{f,b}(t)) dt \quad (4.22)$$

$$T_{mean}(t) = \frac{\sum_k T_i(t) \cdot m_i(t)}{\sum_k m_i(t)} \quad (4.23)$$

Here ω is the engine speed in $\left[\frac{rad}{s}\right]$, p_{O_2} is the partial oxygen pressure of the air-zone in $[bar]$, N' is the engine speed in $[rps]$. C_2 and T_A is assumed to be equal to $1.2 \cdot 10^{10} \left[\frac{K^{0.5}}{bars}\right]$ and $16500 [K]$. T_i and m_i are the temperature and mass for the zone $i = a, p, b$. [2]

In the early stages of combustion the preparation rate, $\dot{m}_{f,p}$, is greater than the burning rate, $\dot{m}_{f,b}$, and with an accumulation of prepared fuel it results in a premixed combustion process. When the energy of the premixed combustion comes to an end, the evaporation and combustion rates are equal and resulting in a mixing-controlled combustion process [3].

4.6 Heat transfer submodel

Figure 4.8 shows which signals that are sent into the submodel and what signals that comes out from the submodel. Two types of heat transfer are

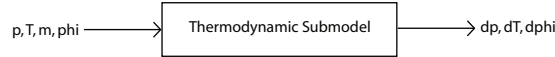


Figure 4.8: In- and outsignals from the heat transfer submodel

discussed in this model; convective heat transfer and radiative heat transfer. The most part of the heat transfer in internal combustion engines comes from convection. This is when heat is transfered through fluids in motion or a fluid and solid surface in relative motion. The *forced convection* is used when the motions are produced by forces other than gravity. In this case there is forced

convection between the in-cylinder gases and the cylinder head, valves, cylinder walls and piston during the different phases. The heat transfer caused by radiation occurs from the high temperature combustion gases and hot particles in the flame region to the combustion chamber walls. The concept of heat transfer by radiation is based on the emission and absorption of electromagnetic waves.[1]

In the burned-zone there are both convective and radiative heat transfer. The total heat transfer in the burned-zone is calculated by the sum as follow:

$$\dot{Q} = \dot{Q}_c + \dot{Q}_r \quad (4.24)$$

The convective heat transfer is described by Newons law of cooling:

$$\dot{Q}_c = h_c A (T - T_w) C_c \quad (4.25)$$

Here T is the temperature in the zone, T_w is the in-cylinder wall temperature, C_c is calibration parameter, A is the in-cylinder area and h_c is given by Woschnis correlation as:

$$h_c = 0.013 \cdot \frac{p^{0.8} \left(C_1 u_p + C_2 \frac{(p-p_m)T_r V}{p_r V_r} \right)^{0.8}}{B^{0.2} \cdot T^{0.55}} \quad (4.26)$$

Here the constants are set to $C_1 = 2.28$ and $C_2 = 0$ during the compression-phase. During the combustion-phase the constants are set as $C_1 = 2.28$ and $C_2 = 3.24 \cdot 10^{-3}$. The other constants and parameters can be seen in table 4.6.

Constant	Description	Unit
u_p	Mean piston speed	$\frac{m}{s}$
B	Cylinder bore	$[m]$
T	Temperature	$[K]$
p_r	Reference pressure	$[P_a]$
V_r	Reference volume	$[m^3]$
T_r	Reference Temperature	$[K]$
p	Fired pressure	$[P_a]$
p_0	Motored pressure	$[P_a]$
C_1	Constant	$[-]$
C_2	Constant	$[\frac{m}{sK}]$

The radiative heat transfer is described by using Stefan-Boltzmann law:

$$\dot{Q}_r = \sigma A (T_b^4 - T_w^4) C_r \quad (4.27)$$

Where σ is Stefan-Boltzmanns constant, C_r is a calibration parameter and T_b is the mean gas temperature in the burned-zone.

Chapter 5

Implementation

This chapter will describe how the model was implemented into the Matlab/Simulink environment. Matlab is a numerical computing environment but also a programming language. Simulink is a tool in Matlab for modeling, simulating and analyzing dynamic systems.

5.1 General view

The entire model consists of all submodels presented in previous chapter and these submodels are implemented in Simulink and a few as S-functions. To simplify the work to implement our multi-zone model has a package called psPack¹ been used. Further information about psPack is presented in section 5.5. The submodels that have been implemented in Simulink contains information that are used by the S-functions² that handles compression and combustion.

5.2 Simulink

Simulink is the environment where all the submodels, presented in the Model theory chapter, was put together to a working unit. Below, in figure 5.1, an example is shown on how the implementation in our model is made, in this case the fuel spray submodel. To the left in the figure is the submodel communicating with all other submodels presented (the top layer). The right part of the figure shows how the fuel spray submodel is built with more submodels that represents different equations (4.15, 4.16, 4.17) in the model.

¹Engine simulation tool developed at Vehicular systems at LiTH

²Internal function in simulink, often written in C- code

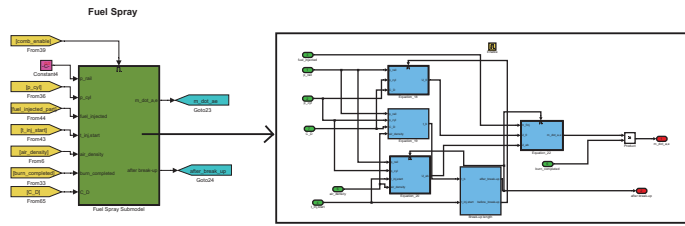


Figure 5.1: A general view of the model to demonstrate how the model is implemented with the different layers in simulink.

5.3 S-functions

In the final model several S-functions have been used. These have been coded in the m-language and are implemented as Level 2 M-file S-Functions. The main S-functions are those who handles the compression and combustion. These S-functions calculates the thermal properties, pressure, temperatures and volumes for the different zones. Some of this information is then feeded back to submodels. There are also S-functions that handles the fuel injection system.

5.4 Solver

To solve the differential equations is a stiff ode³ solver used. The problem is stiff if the solution being sought is varying slowly, but there exists nearby solutions that vary rapidly, so the numerical method must take small steps to obtain satisfactory results.

5.5 psPack

This is a simulation tool that initally was designed for simulation of SI-engines. This package has been stripped down and only the necessary functions are used. In the psPack-menu changes can be made in a few engine parameters such as geometry and engine speed. psPack is allso used to calculate thermal properties for the burned gas. It uses a table where it is looking up the desired thermal property for the current pressure p , temperature T and mass fraction of fuel and air in the zone. This package is developed for Matlab/Simulink.

³Ordinary Differential Equation

5.5.1 Thermal Properties

To calculate the desired thermal property some arguments are sent to the `psPack` function, `psThermProp`, that is needed to interpolate in the tables. As mentioned above it needs p , T and mass fraction of fuel and air for the specific zone. To simplify the call of the thermal property function⁴ the mass fraction are divided as a vector X_{gc} that consists of the fraction of unburned and burned mass of fuel and air. It can be seen in equation 5.1:

$$X_{gc} = (x_{f,u} \quad x_{a,u} \quad x_{f,b} \quad x_{a,b}) \quad (5.1)$$

where $x_{f,u}$ and $x_{a,u}$ stands for the mass fraction in an unburned zone and $x_{f,b}$ and $x_{a,b}$ stands for the same in the burned zone. In our setup of zones there are an air-zone, prepared-zone and a burned-zone. The air-zone is considered as air that is unburned and the prepared-zone is considered as vaporized fuel that also is unburned. In the burned-zone air and vaporized fuel have reacted and there is a mixture of burned fuel and air. Initially there exists a small fraction of burned fuel and air due to residual gas from previously combustion. In equation 5.2 it is shown what the setup of the zones looks like.

$$X_{gc} = \begin{bmatrix} X_{gc,a} \\ X_{gc,p} \\ X_{gc,b} \end{bmatrix} = \begin{bmatrix} 0 & x_{a,u} & 0 & 0 \\ x_{f,u} & 0 & 0 & 0 \\ 0 & 0 & x_{f,b} & x_{a,b} \end{bmatrix} \quad (5.2)$$

where row one is the air-zone, row two is the prepared-zone and row three is the burned-zone.

⁴the function is called `psThermProp()` and is a part of `psPack`

Chapter 6

Validation

In this chapter the validation steps is presented. Validation of the submodels have been carried out in two steps. Both when the submodels are separate units and when they have been put together to one unit.

6.1 Comments about the Validation

The important content of the model is that it should predict torque in a correct way. Unfortunately it is not possible to validate the total model in an good way because the lack of engine measurement data. Although validations of some of the submodels are presented in this chapter. When validations are not possible, experiments have been performed to show that the submodels probably act as it supposed to. With the measurement data thats available can the different submodels behavior be studied in detail. If the submodels behavior is concurrent with the measurement it is probably a good indication that the total model also will concur.

6.2 Fuel injection

The fuel injection is described, as equation (4.12), and is very dependent of the amount of fuel injected hence the parameter C_D change as equation (4.14). A test was formed to show how the parameter C_D affects the mass flow rate at the injection. The test setup can be seen in table 6.1. Figure 6.1 shows the control signal, for the different cases, plotted in the same figure as fuel mass flow rate. As the injected mass increases the parameter C_D changes. These phenomena can be seen as when the first part of the fuel is injected it does not encounter any major resistance. When the amount of fuel increases in the cylinder the later part of the injected fuel encounters a resistance so that it bumps into the aldreedy injected fuel and therefore slows

Injection law set nr	Rail pressure	Injected fuel	N
1	800 [bar]	32.9 [mg]	2500 [rpm]
1	1000 [bar]	36.4 [mg]	2500 [rpm]
1	1200 [bar]	39.4 [mg]	2500 [rpm]

Table 6.1: Table of fuel injection test setup

down the fuel mass flow rate. The resistance that is increased comes from the model of C_D that is described by equation (4.14).

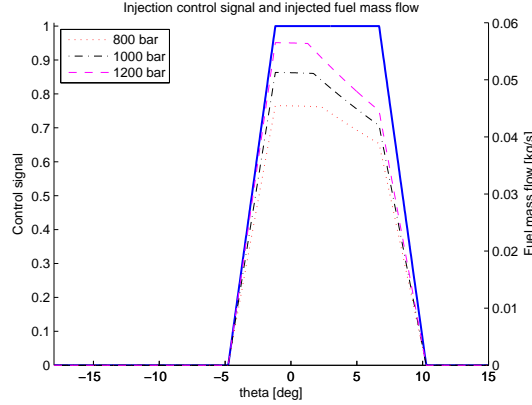


Figure 6.1: Fuel injection control signal and mass flow rate that shows the changes in C_D for different injection pressures. The decrease in C_D can be seen in the decrease of the mass flow after about 2 deg.

6.3 Fuel spray validation

To validate the spray penetration correlation, experimental data collected by Dan et al. [9] were compared with the implemented model predictions. The injection conditions and ambient conditions of the experiment are summarized in Table 6.2. The injector nozzle has a mini-sac volume design for high injection pressure. The injection pressure was varied from 55 MPa to 120 MPa. In figure 6.2 and 6.3 simulations are compared to the measurements of the spray tip penetration as a function of time from start of injection and injection pressure.

In figure 6.2, the measured spray penetration for an injection pressure of 120 MPa is compared with the simulated data from the model. It shows that the implemented model over predicts the spray tip penetration. When the injection pressure is lower, in this case 55 MPa, the model has a better accuracy

Parameter	value/spec
Hole diameter [mm]	0.2
Hole length [mm]	1.1
Number of holes [-]	1
Discharge coefficient of the hole [-]	0.66
Injection pressure [MPa]	55, 120
Ambient pressure [MPa]	1.5
Ambient temperature [K]	293
Ambient density [$\frac{kg}{m^3}$]	17.3
Ambient viscosity [$\cdot 10^{-6} Pa \cdot s$]	17.5

Table 6.2: Experimental setup for the fuel spray validation.

but it still over predicts. This result can be seen in figure 6.3 . This over-prediction probably comes from the disregard of the ambient viscosity in our model that is used in the experimental setup.

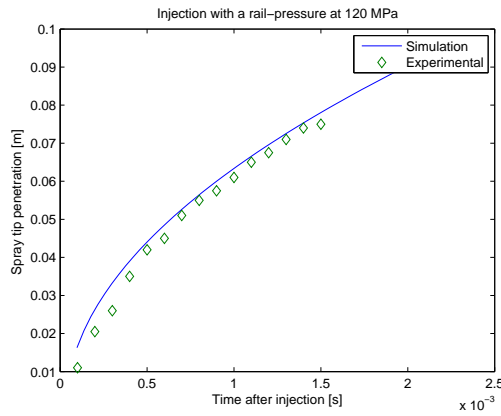


Figure 6.2: Spray tip penetration as function of time with fuel injection pressure 120 MPa. As can be seen the model overpredicts the penetration length slightly.

In figure 6.4 it is shown how the length of the spray tip varies with different sets of rail-pressure. The liquid length is the fuel spray break-up length and is shown as the solid line in the figure. The length of the droplet based spray is the dotted length and the total fuel spray penetration length is the solid and dotted line together. In this simulation was a simulation time of 1.4 millisecond used and the rail pressure was in the four cases 60, 80, 100, 120 MPa.

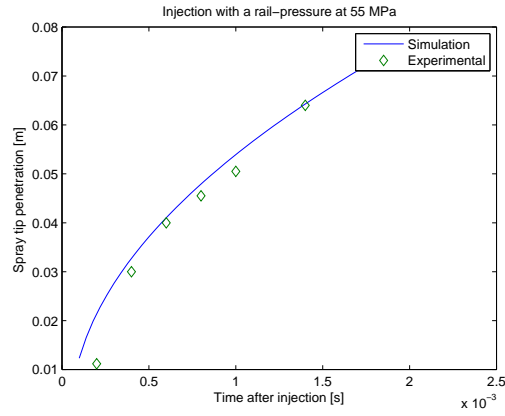


Figure 6.3: Spray tip penetration as function of time with fuel injection pressure 55 MPa. Here it also shown that the model slightly overpredict the penetration length.

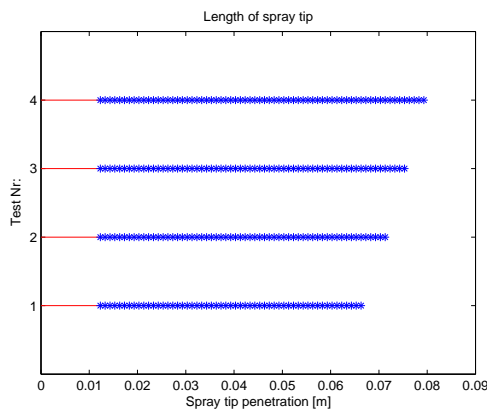


Figure 6.4: Spray tip length, for different injection pressures. From the top: 120, 100, 80, 60 MPa. The solid line represents liquid length. As expected the penetration is larger for higher pressures.

6.4 Fuel evaporation model

To validate the fuel evaporation model the injected fuel mass and the mass of the evaporated fuel are plotted in the same plot. Figure 6.5 shows the injection and evaporation of fuel with only a main injection. It is shown that the evaporation process looks like a first order system and this seems to be correct when a comparison is made between these plots and the plots presented in the Salerno rapport [2]. In figure 6.6 is a new simulation made with the difference that both pre- and main injection is used.

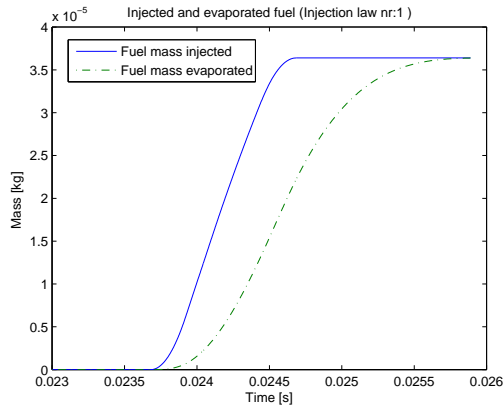


Figure 6.5: Fuel injection and evaporation, main injection (injection law nr 1). The shape of the evaporated mass is consistent with a first order system and the result is similar to the result in [2].

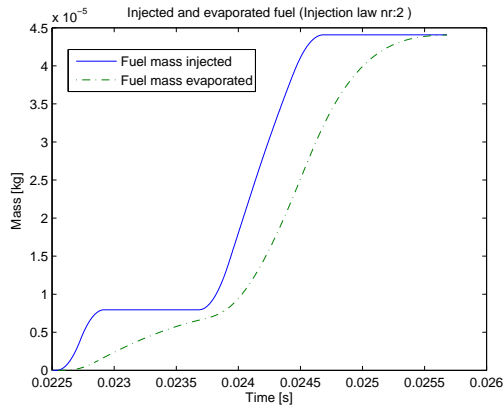


Figure 6.6: Fuel injection and evaporation, pre + main injection (injection law nr 2). When using multiple injections the evaporated mass is still consistent with a first order system.

In the following figure it's presented how the rate of evaporation varies during the injection. In figure 6.7 the rate for both injection law one and two is plotted, see Table 6.5 for more information.

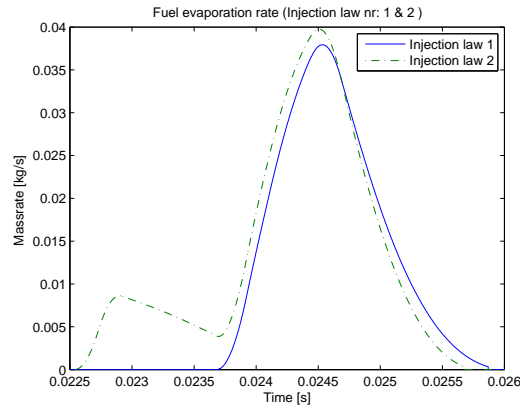


Figure 6.7: Fuel evaporation rate for injection law nr 1 plotted with injection law 2. This shows how the fuel evaporation rate varies during two different types of injections.

6.5 Evaporation and combustion submodel

In the model the atomization of fuel into droplets, vaporization of the fuel, entrainment of air and micromixing of fuel and air are joint together and is known as preparation of fuel according to the equations (4.21,4.22). At the start of the combustion the fuel burning rate is lower than the preparation rate. As the prepared fuel is accumulated it causes an increase in the burning rate. Then, as the combustion proceeds, the burning rate increases faster than the preparation rate. When the prepared fuel is depleted the burning rate is decreasing. This is a result of premixed combustion process and the burning rate is controlled by the chemical kinetics.[3]

To validate the premixing combustion process a test setup in table 6.3 was used.

Start of injection	Fuel injected
$\theta = 4.76 \text{ deg BTDC}$	21.56 [mg]

Table 6.3: Test setup for evaporatin and combustion validation.

In figure 6.8 it's shown that this premixed behaviour starts at 4 [deg] BTDC and ends at 4 [deg] ATDC. After the premixed behaviour is completed the mixing controlled combustion starts. As a result of the mixing controlled combustion process the combustion and preparation rate keeps equal to the

end of the combustion. In the same figure it can be seen that the mixing controlled combustion process proceed after 4 [deg] ATDC and ending at 27 [deg] ATDC.

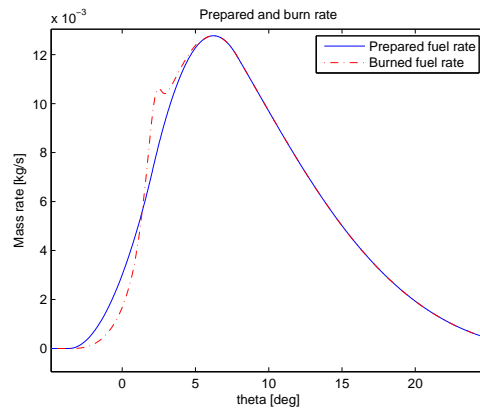


Figure 6.8: Mass flow rate for prepared-zone and combustion-zone. The premixed behaviour can be seen between 4 BTDC and 4 ATDC. After that the mixing controlled combustion starts.

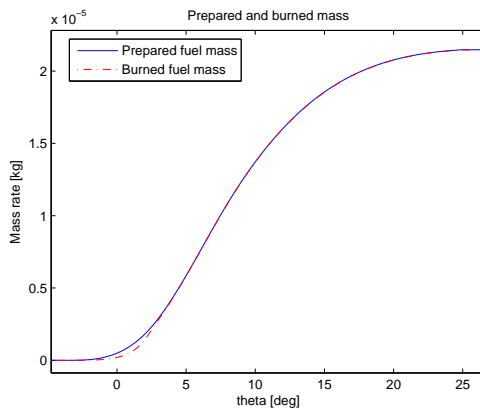


Figure 6.9: Inserted mass for prepared and combusted fuel. As seen in figure the shape of the cumbusted fuel is consistent with a first order system.

In figure 6.9 it is shown that the prepared mass and burned mass behave like a first order system. The equations (4.21) and (4.22) prove that this is a correct behavior. In equation (4.22) it is clear that the early stages in the combustion

is controlled by an Arrhenius ¹ like part. This part describes the temperature dependence of the rate of chemical reaction. It can also be considered to represent the ignition delay time. The constant C_2 also controls the ignition delay time. In the simulation of the burning rate is the end of combustion considered as when the burned fuel fraction reaches 0.9995, as described in equation (6.1):

$$\frac{m_{f,b}}{m_{f,inj}} \geq 0.9995 \quad (6.1)$$

6.6 Heat transfer model

In this section the implemented heat transfer model is validated. In table 6.3 the setup for this validation is presented. Figure 6.10 shows how the convective and radiative heat transfer varies during the combustion process. Lack of validation data will force to validate the model just by looking at the fundamental appearance of the heat transfer curves. The figure also shows that the convective heat transfer stands for the largest part of the total heat transfer. When the combustion starts, just before TDC, the radiative heat transfer increases, and is at most about 30 percent of the total heat transfer.

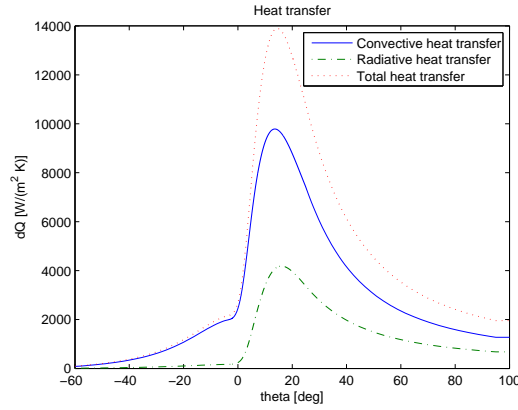


Figure 6.10: Total heat transfer for a simulation. In figure it is show that the largest part for the heat transfer originates from convective heat transfer.

¹The Arrhenius equation is a simple, but remarkably accurate, formula for the temperature dependence of the rate constant, and therefore rate, of a chemical reaction

6.7 Thermal properties

One important part of model accuracy is to have correct values for the thermal properties of the different zones. There exist a program called Chepp² which calculates the thermal properties for different types of zones. Unfortunately this program could not be used in the final product. Tables are used as a replacement to obtain the desired thermal property for the specific mass fraction of air and fuel ($x_{f,u}$, $x_{a,u}$, $x_{f,b}$, $x_{a,b}$), T and p . If some value is going out of bound the tables extrapolates.

In figure 6.11 6.12 6.13 it is shown that the table calculations fit the calculations produced from Chepp. These calculations have been made for an unburned zone where x_f vary from 0 to 1. To to get a clearer view the calculations for the tables have been downsampled.

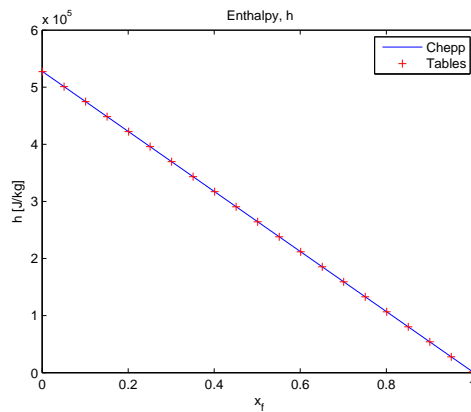


Figure 6.11: Comparison between Chepp and tables for calculation of enthalpy. It is shown that the values from generated from tables correspond very well to the values produced from Chepp.

6.8 Heat release analysis

In this section two experiment are made to validate the heat release. The heat release rate for the experiment is given by real measurments from GM. The heat release for the simulated model is approximated with the fuel burn rate e.g. \dot{m}_{fb} . In table 6.4 the model parameters that is used in the simulation is presented.

²Chemical Equilibrium Program, developed at Vehicular systems by Lars Eriksson

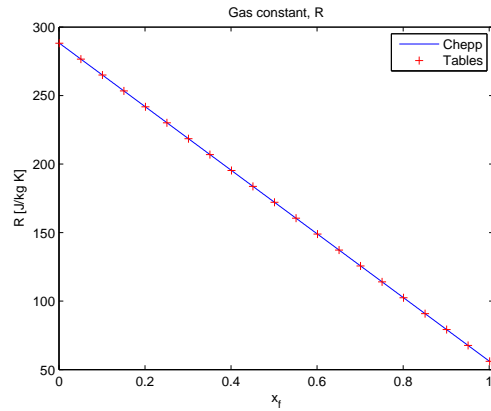


Figure 6.12: Comparison between Chepp and tables for calculation of the gas constant. As seen in figure 6.11 the values from tables in this figure correspond very well to values from Chepp.

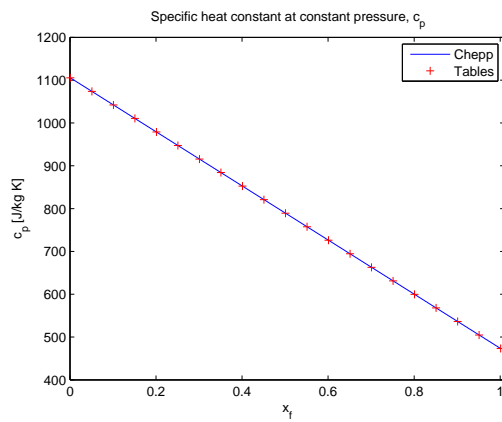


Figure 6.13: Comparison between Chepp and tables for calculation of c_p . As figure 6.11 and 6.12 the values from tables in this figure correspond very well to values from Chepp.

In figure 6.14 and 6.15 the heat release rate from experimental data versus the simulated burn rate is presented. In the figures are the levels matched just to get a good appearance because the interest is only when the peaks occurs. The highest peak in figure 6.14 and 6.15 for the heat release rate starts just before TDC and is also the same for the burn rate.

The model parameter T_A has been set to 20500 to match the experimental data. In figure 6.16 a sensitivity analysis is shown, where the parameter T_A varies with $\pm 10\%$. This figure represents experimental data one and the figure

Variable	Value	Unit
T_{im}	325	[K]
T_{res}	440,480	[K]
x_{res}	33	[%]
T_A	20500	[K]

Table 6.4: Setup for heat release experiment one and two.

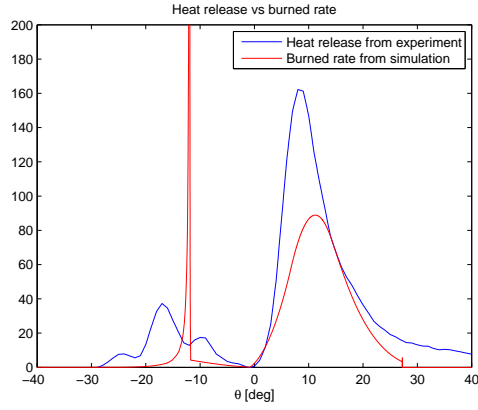


Figure 6.14: Heat release for experiment one. As can be seen in figure the timing of heat release and the burned-rate is matched good, around TDC.

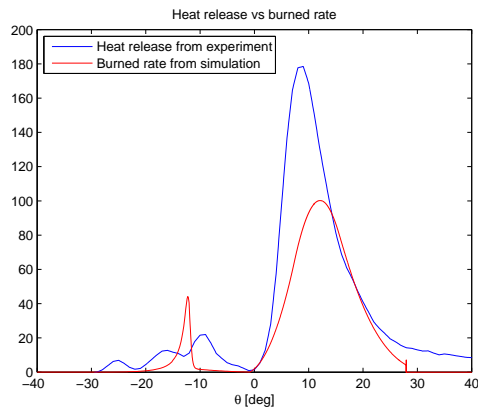


Figure 6.15: Heat release for experiment two. As can be seen in figure the timing of heat release and the burned-rate is matched good, around TDC.

for experimental data two is located in Appendix B. It shows that an increase in the parameter T_A postpone the first burn rate peak and a decrease in the

same parameter moves the first burn rate peak earlier. The position of the main peak is not affected of changes in T_A . This is because that the combustion already has started and when the second injection occurs it ignites at once. This means that evaporation rate and combustion rate is the same after the first injection.

An sensitivity analysis has also been performed in the parameter T_{res} . The parameter varies with $\pm 10\%$ and the figures are located in Appendix B.

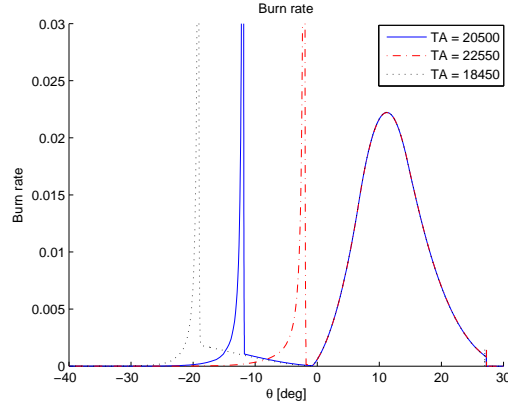


Figure 6.16: Burnrate for different T_A in experiment two. Experiment varies with $\pm 10\%$ in the parameter and shows that the peak can be placed further from or closer to the main injection.

6.9 Pressure

Figure 6.17 and 7.1 shows the pressure trace from our model compared with experimental data number one. In figure 6.17 it shows that the model predicts the pressure in a good way. However the top pressure is over estimated with about 5 bar.

In figure 6.18 the pressure trace from experimental data two is compared with the simulated model. In this work point³ the top pressure is even more over estimated and the first pressure top that occurs at TDC is heavily under estimated. This is shown in figure 6.18.

³i.e rpm and load

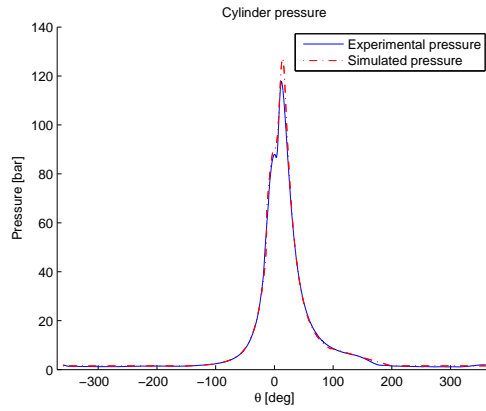


Figure 6.17: Pressure-trace for experiment one. It is shown that the simulated pressure is slightly under predicted at TDC and slightly over predicted a few degrees after TDC.

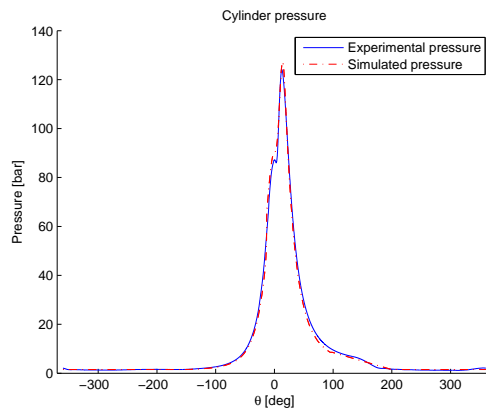


Figure 6.18: Pressure-trace for experimental setup two. The under and over prediction of the simulated pressure is a bit larger than seen in figure 6.17.

6.10 In-cylinder temperature

To show the effects of pre-injection a test set was constructed, see table 6.5.

In figure 6.19 the temperature in the burned-zone is plotted against the crank angle, evidencing an minor increase of the maximum temperature in the test case with only one main injection. In the presence of pre and main injection, test case 2, the maximum temperature is reduced. This reduction is achieved due to the reduced mass of fuel of the main injection, although the same amount of injected fuel is the same in both test cases.

Injection type	Inj 1	Inj 2
Only main	-	$\left\{ \begin{array}{l} \theta_{start}=7 \text{ deg } BTDC \\ m_{inj}=15.37[mg] \end{array} \right\}$
Pre- and main	$\left\{ \begin{array}{l} \theta_{start}=25.7 \text{ deg } BTDC \\ m_{inj1}=2.76[mg] \end{array} \right\}$	$\left\{ \begin{array}{l} \theta_{start}=7 \text{ deg } BTDC \\ m_{inj2}=12.65[mg] \end{array} \right\}$

Table 6.5: Table of injection law sets. The two different injections has the same total amount of injected fuel.

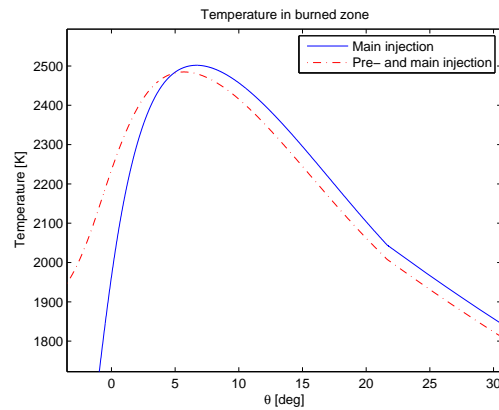


Figure 6.19: Difference between temperature in the burned zone. It is shown that a injection law with pre + main injection may reduce the high temperature.

The IMEP⁴ is almost the same for the two cases (14.12, 14.5) bar. This is evidencing that the occurrence of pre-injection may reduce the maximum temperature while keeping almost the same IMEP, with benefits of lower NO_x emissions. These is the same conclusions that is made in (Arise et al., 2005) [2].

⁴Indicated Mean Effective Pressure

Chapter 7

Results and Conclusions

In this chapter the results and conclusions that can be recognised are presented.

7.1 Results

Below are data from our model presented and compared with experimental data. Two figures are also shown to help illustrate the performance of the model. In table 7.1 it is shown that our model can predict the torque during one cycle that only differ 0.7 % with experimental data (Experimental setup one). In table 7.1 it is shown that our model gives a mean square error between 0.36 - 0.80 Nm.

Experimental setup	Measurement	Simulated	Experimental
One	Torque [Nm]	59.9881	59.5284
One	IMEP [Bar]	10.7443	11.1063
Two	Torque [Nm]	53.7677	54.9965
Two	IMEP [Bar]	10.3045	10.5152

Table 7.1: Results presented for both experiment one and two.

Experimental setup	Measurement	Result
One	Mean fault [Nm]	0.362064
Two	Mean fault [Nm]	0.801828

Table 7.2: Results presented for both experiment one and two.

Figures 7.1 and 7.2 shows a comparison between measurement data and experimental data for the two different setups. This is presented with the help of

pV-diagrams. The figures shows that the model gives a good approximation of the pressure during a whole combustion cycle.

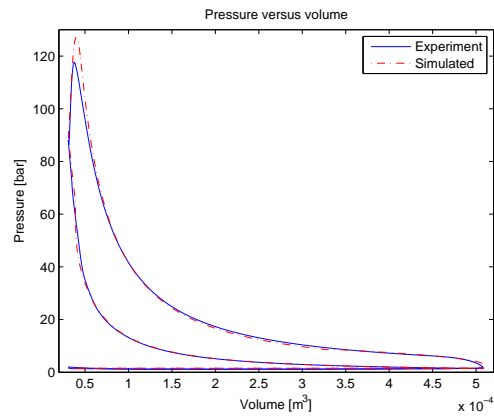


Figure 7.1: Pressure versus volume (pV-plot) for experiment one. In this pV-plot the over prediction of top-pressure is shown.

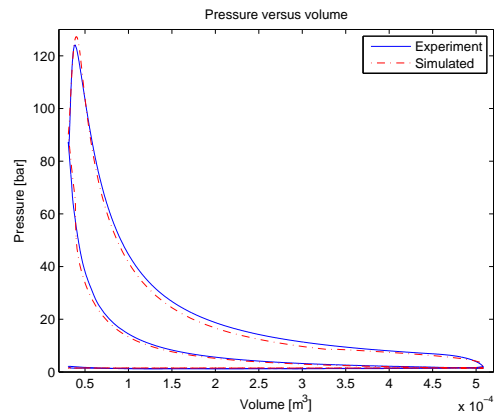


Figure 7.2: Pressure versus volume (pV-plot) for experiment two. In this pV-plot the over prediction of top-pressure is shown.

7.2 Conclusions

- A model that can predict the engine torque has been implemented.

- The validation in the two engine operating-points gives a good result when comparing the implemented model and the engine measurement data.
- Since a complete validation not has been possible to accomplish the different submodels has been investigated separately. The submodels that were possible to validate have been validated with good result.
- For those submodels that not have been possible to validate experiments have been constructed to show that the submodel is very likely to behave in a correct manner.
- A sensitivity analysis has been performed for some of the ingoing model parameters.
- Together with the sensitivity analysis and the investigation of the ingoing submodels the results show that the parts that need more validation is fuel injection and heat transfer and while the the models for evaporation, combustion and fuel spray indicates a satisfying result.

7.3 Future work

The existing model that has been presented in this thesis can be further modified and improve in the following items:

- **Gas exchange model.** To get the full pressure trace it is necessary to have an accurate gas exchange model.
- **Swirl model.** To get a more accurate model of the fuel spray distribution it should be considered to model the swirl factor. The swirl factor is a measurement of how turbulent the airflow is in the combustion chamber.
- **Advanced model of fuel spray.** Another step to increase accuracy in the model is to divide the fuel spray into several zones and consider droplet distribution. This is a more advanced fuel spray model and is proposed by Jung, Assanis [4].
- **Wall wetting.** There may occur injections where the injected fuel hits the in-cylinder wall and cools down which prevents the evaporation process to happen.

- **Cylinder wall temperature** Examine how the changes in the in-cylinder wall temperature effects the combustion process.
- **Parameter identification** To enhance the accuracy in the model further work in tuning and verifying the parameters must be done.

If some of these improvements is done the complexity increases and therefore the computational time and simulation time will increase.

Chapter 8

References

- [1] John B. Heywood. *Internal Combustion Engine Fundamentals*. McGraw-Hill Book Co, 1988.
- [2] C. Pianese G. Rizzo A. Caraceni P. Cioffi G. Flauti I. Arsie. *Thermodynamic modeling of jet formation and combustion in common rail multi-jet diesel engines*. SAE Thechnical Papers Series 2005-01-1121, 2005.
- [3] J. I. Ramos. *Internal Combustion Engine Modeling*. Hemisphere Publishing Corporation, 1989.
- [4] Dohoy Jung and Dennis N. Assanis. *Multi-Zone DI Diesel Spray Combustion Model for Cycle Simulation Studies of Engine Performance and Emissions*. SAE Technical Papers Series 2001-01-1246, 2001.
- [5] L. Eriksson Y. Nilsson. *A new formulation of multizone combustion engine models*. Internal technical report. Department of Electrical Engineering, Linköpings University.
- [6] L. Eriksson L Nielsen. *Vehicular Systems*. Technical report. Department of Electrical Engineering, Linköpings University, 2006.
- [7] C. F. Taylor. *The Internal-Combustion Engine in Theory and Practice, Revised Edition*. The M.I.T press, Seventh printing, 1995.
- [8] C. Argachoy. A. P. Pimenta. *Phenomenological Model of Particulate Matter Emission from Direct Injection Diesel Engines*. Technical Paper. 2005.
- [9] J. Senda H. Fujimoto T. Dan. S. Takagishi. *Effect of ambient gas properties for characteristics of non-reacting diesel fuel spray*. SAE Technical Paper Series 9703552, 1997.

- [10] *Nationalencyklopedin*, 2007
- [11] [http : //auto.howstuffworks.com/diesel1.htm](http://auto.howstuffworks.com/diesel1.htm), October 2008
- [12] Y. Kim, J. Lim, and K. Min *A study of the dimethyl ether spray characteristics and ignition delay* School of Mechanical and Aerospace Engineering, Seoul National University, April 2007
- [13] P. Öberg *A DAE Formulation and it's Numerical Solution for Multi-Zone thermodynamic models* Technical report in progress. Department of Electrical Engineering, Linköpings University, 2008

Notation

Symbols used in the report.

Variables and parameters

C_D	Discharge coefficient	[-]
m	Mass	kg
$m_{f,b}$	Mass of burned fuel	kg
$m_{f,p}$	Mass of prepared fuel	kg
$m_{f,inj}$	Mass of fuel injected	kg
$m_{a,e}$	Mass of air entrained	kg
N	Engine speed	rev/s
N'	Engine speed	rad/s
p_{atm}	Atmospheric normal pressure	Pa
p_{rail}	Rail Pressure	Pa
p_{cyl}	Cylinder Pressure	Pa
R	Gas constant	J/(kgK)
S_{break}	Break-up length	m
t	Time from start of injection	s
t_{break}	Fuel spray break-up time	s
$t_{inj,d}$	Fuel spray break-up time	s
T	Temperature	K
T_w	Cylinder wall temperature	K
V	Volume	m^3

Appendix A

Derivation of air entrainment rate and thermodynamic model

In this chapter the derivation of air entrainment rate and thermodynamic model that is used in the report is presented.

A.1 Air entrainment rate

The prediction of the entrained air is based on the conservation of momentum. It assumes that the initial momentum imparted by the fuel flow at the nozzle exit is equal to the sum of the momentum of the unburned and liquid zone as:

$$m_{f,inj} \cdot U_0 = (m_{f,inj} + m_{a,e}) U_{spray} \quad (A.1)$$

where $m_{f,inj}$ is the fuel injected, $m_{a,e}$ is the entrained air, U_0 is the fuel flow velocity at the nozzle exit considered constant value and U_{spray} is the fuel spray velocity. Equation A.1 can be rewritten as:

$$m_{a,e} = m_{f,inj} \left(U_0 \frac{1}{U_{spray}} - 1 \right) \quad (A.2)$$

Then by differentiating equation A.2 with respect to time, the air entrainment rate come out as:

$$\dot{m}_{a,e} = - \frac{\int_0^t \dot{m}_{f,inj}(t) dt \cdot U_0}{(U_{spray}(t))^2} \cdot \dot{U}_{spray}(t) \quad (A.3)$$

which is the expression we use in air entrainment section.

A.2 Thermodynamic Equations

A.2.1 Energy at equilibrium

The change in energy for an open system are described by the equations below. **Note** that the function for the different parts x_k can vary from zone to zone and that $x_{j,k}$ is used to denote that it is the x_k -function for the source j that's regarded. The index b,e denote *beginning* and *end* respectively.

$$\Delta U = \Delta W + \Delta Q \quad (\text{A.4})$$

$$U_b = m \sum_k x_k(p_b, T_b, \bar{x}_{r,b}) u_k(T_b) + \Delta m_j \sum_k \hat{x}_{j,k}(p_b, \hat{T}_j, \hat{\bar{x}}_{r,j}) u_k(\hat{T}_j) \quad (\text{A.5})$$

$$\begin{aligned} U_e &= (m + \Delta m_j) \sum_k x_k(p_e, T_e, \bar{x}_{r,e}) u_k(T_e) = \\ &= (m + \Delta m_j) \sum_k x_k(p_b + \Delta p, T_b + \Delta T, \bar{x}_{r,b} + \Delta \bar{x}_r) u_k(T_b + \Delta T) = \\ &= (m + \Delta m_j) \sum_k \left(x_k(p_b, T_b, \bar{x}_{r,b}) + \frac{\partial x_k}{\partial p} \Delta p + \frac{\partial x_k}{\partial T} \Delta T + \right. \\ &\quad \left. + \nabla_{\bar{x}_r} x_k \cdot \Delta \bar{x}_r + O(\Delta^2) \right) \left(u_k(T_b) + \frac{\partial u_k}{\partial T} \Delta T + O(\Delta^2) \right) = \\ &= m \sum_k x_k(p_b, T_b, \bar{x}_{r,b}) u_k(T_b) + m \sum_k \left(\frac{\partial x_k}{\partial p} \Delta p + \frac{\partial x_k}{\partial T} \Delta T + \nabla_{\bar{x}_r} x_k \cdot \Delta \bar{x}_r \right) u_k(T_b) + \\ &\quad + m \sum_k x_k(p_b, T_b, \bar{x}_{r,b}) \frac{\partial u_k}{\partial T} \Delta T + \Delta m_j \sum_k x_k(p_b, T_b, \bar{x}_{r,b}) u_k(T_b) + O(\Delta^2) \end{aligned} \quad (\text{A.6})$$

$$\begin{aligned} \Delta U = U_e - U_b &= m \sum_k \left(\frac{\partial x_k}{\partial p} \Delta p + \frac{\partial x_k}{\partial T} \Delta T + \nabla_{\bar{x}_r} x_k \cdot \Delta \bar{x}_r \right) u_k(T_b) + \\ &\quad + m \sum_k x_k(p_b, T_b, \bar{x}_{r,b}) \frac{\partial u_k}{\partial T} \Delta T + \\ &\quad + \Delta m_j \sum_k \left(x_k(p_b, T_b, \bar{x}_{r,b}) u_k(T_b) - \hat{x}_{j,k}(p_b, \hat{T}_j, \hat{\bar{x}}_{r,j}) u_k(\hat{T}_j) \right) \end{aligned} \quad (\text{A.7})$$

Divide with Δt , and let $\Delta t \rightarrow 0$, dump dt , replace $\{\}_b$ with $\{\}$ and separate the work done by the gas on the zone and the work originating from the internal change of volume.

Hence:

$$dU = dQ - pdV + dm_j p v_j \quad (\text{A.8})$$

$$\begin{aligned} dU = m \sum_k \left(\frac{\partial x_k}{\partial p} dp + \frac{\partial x_k}{\partial T} dT + \nabla_{\bar{\mathbf{x}}_r, x_k} \cdot d\bar{\mathbf{x}}_r \right) u_k(T) + \\ + m \sum_k x_k(p, T, \bar{\mathbf{x}}_r) \frac{\partial u_k}{\partial T} dT + \\ + dm_j \sum_k \left(x_k(p, T, \bar{\mathbf{x}}_r) u_k(T) - \hat{x}_{j,k}(p, \hat{T}_j, \hat{\bar{x}}_{r,j}) u_k(\hat{T}_j) \right) \end{aligned} \quad (\text{A.9})$$

There

$$\hat{\chi}_j = \begin{cases} \chi_j & \text{For flow from outside to inside } (dm_j > 0) \\ \chi & \text{For flow from inside to outside } (dm_j \leq 0) \end{cases}$$

For $\chi \in \{T, \bar{\mathbf{x}}_r, x_k\}$.

A.2.2 Energy with a frozen mixture

The difference between an equilibriumstate mixture and a frozen mixture is the x_k function in the zone. For a frozen mixture the x_k is not dependent on the pressure nor the temperature but it is dependent on the particles that flows in.

In the same way as above in the equilibrium state we have:

$$\Delta U = \Delta W + \Delta Q U_b = m \sum_k x_{k,b} u_k(T_b) + \Delta m_j \sum_k \hat{x}_{j,k} u_k(\hat{T}_j) \quad (\text{A.10})$$

$$\begin{aligned} U_e = (m + \Delta m_j) \sum_k x_{k,e} u_k(T_e) &= (m + \Delta m_j) \sum_k (x_{k,b} + \Delta x_k) u_k(T_b + \Delta T) = \\ &= (m + \Delta m_j) \sum_k (x_{k,b} + \Delta x_k) \left(u_k(T_b) + \frac{\partial u_k}{\partial T} \Delta T + O(\Delta^2) \right) = \\ &= m \sum_k x_{k,b} u_k(T_b) + m \sum_k x_{k,b} \frac{\partial u_k}{\partial T} \Delta T + \\ &\quad + m \sum_k \Delta x_k u_k(T_b) + \Delta m_j \sum_k x_{k,b} u_k(T_b) + O(\Delta^2) \end{aligned} \quad (\text{A.11})$$

$$\begin{aligned} \Delta U = U_e - U_b &= m \sum_k x_{k,b} \frac{\partial u_k}{\partial T} \Delta T + m \sum_k \Delta x_k u_k(T_b) + \\ &\quad + \Delta m_j \sum_k \left(x_{k,b} u_k(T_b) - \hat{x}_{j,k} u_k(\hat{T}_j) \right) + O(\Delta^2) \end{aligned} \quad (\text{A.12})$$

$$\Delta x_k = x_{k,f} - x_{k,b} = \frac{m x_{k,b} + \Delta m_j \hat{x}_{j,k}}{m + \Delta m_j} - \frac{(m + \Delta m_j) x_{k,b}}{m + \Delta m_j} = \frac{\Delta m_j (\hat{x}_{j,k} - x_{k,b})}{m + \Delta m_j} \quad (\text{A.13})$$

Divide with Δt , and let $\Delta t \rightarrow 0$, dump dt , replace $\{\}_b$ with $\{\}$ and separate the work done by the gas on the zone and the work originating from the internal change of volume.

Hence:

$$dU = dQ - pdV + dm_j p v_j \quad (\text{A.14})$$

$$dU = m \sum_k dx_k u_k(T) + m \sum_k x_k \frac{\partial u_k}{\partial T} dT + dm_j \sum_k \left(x_k u_k(T) - \hat{x}_{j,k} u_k(\hat{T}_j) \right) \quad (\text{A.15})$$

$$dx_k = \frac{1}{m} (\hat{x}_{j,k} - x_k) dm_j \quad (\text{A.16})$$

Here are

$$\hat{\chi}_j = \begin{cases} \chi_j & \text{For flow from outside to inside } (dm_j > 0) \\ \chi & \text{For flow from inside to outside } (dm_j \leq 0) \end{cases} \quad (\text{A.17})$$

For $\chi \in \{T, \bar{\mathbf{x}}_r, x_k\}$.

A.2.3 State equation - the ideal gas law

For both the *well stirred reactor*- and the *well stirred mixer* -case the state equation looks like as follows:

$$\left. \begin{aligned} pV &= n(p, T, \bar{\mathbf{x}}) \tilde{R} T \\ n &= \sum_k n_k = \sum_k x_k \frac{m}{M_k} \end{aligned} \right\} \Rightarrow \quad (\text{A.18})$$

$$pV = m \sum_k \frac{x_k(p, T, \bar{\mathbf{x}}_r) \tilde{R}}{M_k} T = m R(\bar{\mathbf{x}}(p, T, \bar{\mathbf{x}}_r)) T$$

The following relations can now be considered:

$$pdV + V dp = R(\bar{\mathbf{x}}(p, T, \bar{\mathbf{x}}_r)) T dm_j + m R(\bar{\mathbf{x}}(p, T, \bar{\mathbf{x}}_r)) dT + m T dR \quad (\text{A.19})$$

there

$$\begin{aligned} dR &= \frac{\partial R}{\partial p} dp + \frac{\partial R}{\partial T} dT + \nabla_{\bar{\mathbf{x}}_r} R \cdot d\bar{\mathbf{x}}_r = \\ &= \frac{\partial R}{\partial p} dp + \frac{\partial R}{\partial T} dT + \nabla_{\bar{\mathbf{x}}_r} R \cdot \frac{1}{m} (\hat{\mathbf{x}}_{r,j} - \bar{\mathbf{x}}_r) dm_j \end{aligned} \quad (\text{A.20})$$

That leads to:

$$pdV + V dp = R T dm_j + m R dT + T \left(m \frac{\partial R}{\partial p} dp + m \frac{\partial R}{\partial T} dT + \nabla_{\bar{\mathbf{x}}_r} R \cdot (\hat{\mathbf{x}}_{r,j} - \bar{\mathbf{x}}_r) dm_j \right) \quad (\text{A.21})$$

Equation A.21 is used as state equation for both *well stirred reactor* and *well stirred reactor*.

Appendix B

Sensitivity plots

This chapter presents a sensitivity analysis of the two parameters T_{res} and T_A .

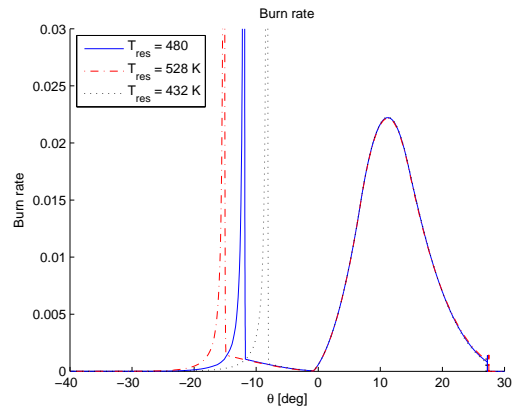


Figure B.1: Burnrate for different T_{res} in experiment one. Variation in parameter is $\pm 10\%$. It is shown that temperature of the residual gas is affecting the position for the first peak of burn-rate.

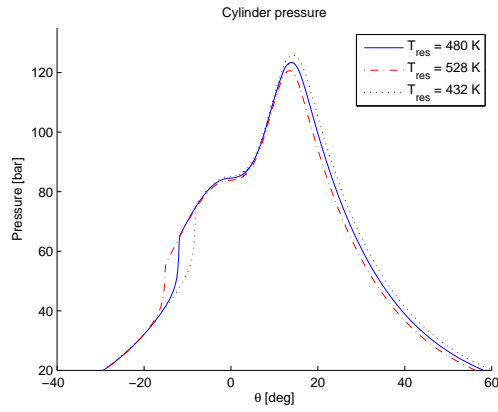


Figure B.2: Pressure for different T_{res} in experiment one. Variation in the parameter is $\pm 10\%$. It can be seen that a lower residual gas temperature can delay the combustion, raise the top pressure and also hold the pressure slightly higher after the top pressure.

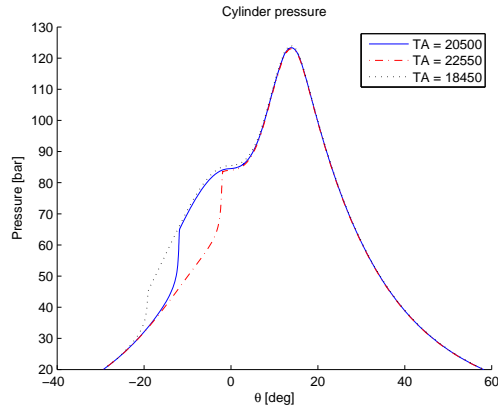


Figure B.3: Pressure for different T_A in experiment one. Variation in the parameter is $\pm 10\%$. Here it is shown that the parameter is affecting the timing of the combustion. The top pressure is almost the same for the three cases.

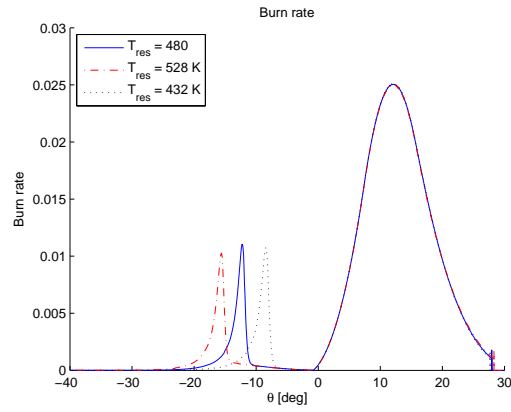


Figure B.4: Burnrate for different T_{res} in experiment two. It is shown that temperature of the residual gas is affecting the position for the first peak of burn-rate.

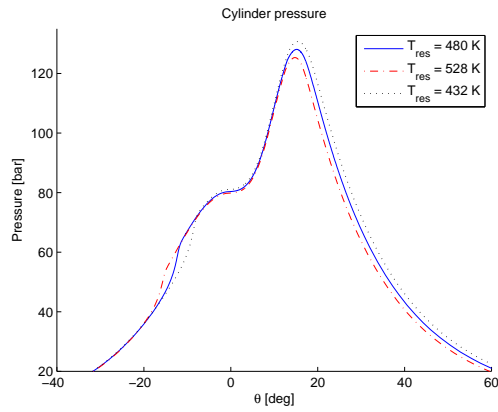


Figure B.5: Pressure for different T_{res} in experiment two. Variation in the parameter is $\pm 10\%$. It can be seen that a higher residual gas temperature can start the combustion earlier, decrease the top pressure and also hold the pressure slightly lower after the top pressure.

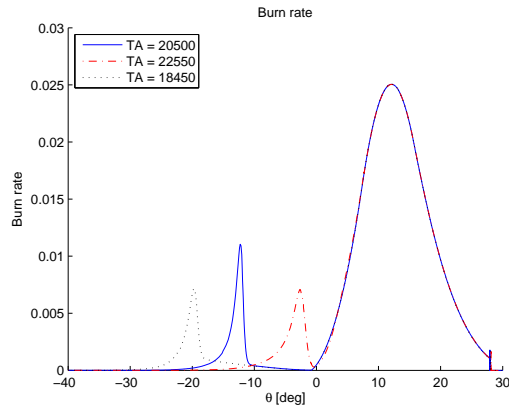


Figure B.6: Burnrate for different T_A in experiment two. Experiment varies with $\pm 10\%$ in the parameter and shows that the first peak can be placed further from or closer to the main injection.

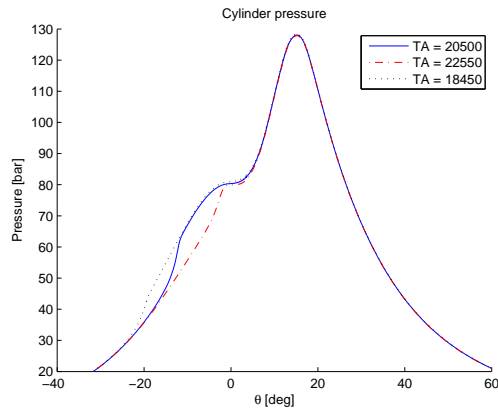


Figure B.7: Pressure for different T_A in experiment two. Variation in the parameter is $\pm 10\%$. Here it is shown that the parameter is affecting the timing of the combustion. The top pressure is almost the same for the three cases.

Copyright

Svenska

Detta dokument hålls tillgängligt på Internet - eller dess framtida ersättare - under en längre tid från publiceringsdatum under förutsättning att inga extraordinära omständigheter uppstår.

Tillgång till dokumentet innebär tillstånd för var och en att läsa, ladda ner, skriva ut enstaka kopior för enskilt bruk och att använda det oförändrat för icke-kommersiell forskning och för undervisning. Överföring av upphovsrätten vid en senare tidpunkt kan inte upphäva detta tillstånd. All annan användning av dokumentet kräver upphovsmannens medgivande. För att garantera äktheten, säkerheten och tillgängligheten finns det lösningar av teknisk och administrativ art.

Upphovsmannens ideella rätt innefattar rätt att bli nämnd som upphovsman i den omfattning som god sed kräver vid användning av dokumentet på ovan beskrivna sätt samt skydd mot att dokumentet ändras eller presenteras i sådan form eller i sådant sammanhang som är kränkande för upphovsmannens litterära eller konstnärliga anseende eller egenart.

För ytterligare information om Linköping University Electronic Press se förlagets hemsida: <http://www.ep.liu.se/>

English

The publishers will keep this document online on the Internet - or its possible replacement - for a considerable time from the date of publication barring exceptional circumstances.

The online availability of the document implies a permanent permission for anyone to read, to download, to print out single copies for your own use and to use it unchanged for any non-commercial research and educational purpose. Subsequent transfers of copyright cannot revoke this permission. All other uses of the document are conditional on the consent of the copyright owner. The publisher has taken technical and administrative measures to assure authenticity, security and accessibility.

According to intellectual property law the author has the right to be mentioned when his/her work is accessed as described above and to be protected against infringement.

For additional information about the Linköping University Electronic Press and its procedures for publication and for assurance of document integrity, please refer to its WWW home page: <http://www.ep.liu.se/>

© Fredrik Jones, Christoffer Jezek
Linköping, June 11, 2008